

Contingency Analyses with Warm Starter using Probabilistic Graphical Model

Shimiao Li, *Graduate Student Member, IEEE*, Amritanshu Pandey, *Member, IEEE*,
and Larry Pileggi, *Fellow, IEEE*

Abstract—Cyberthreats are an increasingly common risk to the power grid and can thwart secure grid operation. We propose to extend contingency analysis (CA) that is currently used to secure the grid against natural threats to protect against cyberthreats. However, unlike traditional N-1 or N-2 contingencies, cyberthreats (e.g., MadIoT) require CA to solve harder N-k (with $k \gg 2$) contingencies in a practical amount of time. Purely physics-based solvers, while robust, are slow and may not solve N-k contingencies in a timely manner, whereas the emerging data-driven alternatives to power grid analytics are fast but not sufficiently generalizable, interpretable, or scalable. To address these challenges, we propose a novel conditional Gaussian Random Field-based data-driven method that is both fast and robust. It achieves speedup by improving starting points for the physical solvers. To improve the physical interpretability and generalizability, the proposed method incorporates domain knowledge by considering the graphical nature of the grid topology. To improve scalability, the method applies physics-informed regularization that reduces the model size and complexity. Experiments validate that simulating MadIoT-induced N-k contingencies with our warm starter requires 5x fewer iterations for a realistic 2000-bus system.

Index Terms—contingency analysis, graph neural network, Gaussian random field, MadIoT, physics informed machine learning, power flow, warm start

I. INTRODUCTION

The power grid is becoming increasingly challenging to operate. Climate change is accelerating the frequency of natural disasters, causing a higher rate of equipment failure, and new-age grid resources such as renewables and distributed energy resources are causing more uncertainty in supply. Amid the growing uncertainties and threats, today's grid operators use contingency analysis (CA) to identify the grid's vulnerability against them.

CA [1] is a simulation module located within the grid control centers' Energy Management System (EMS). Grid operators (and planners) use it to perform a set of "what if" power flow simulations to preemptively evaluate the impacts of selected disturbances and outages on the power grid health indicators (e.g., voltages and line flow). If the output from CA indicates that the grid is operating in an unstable state, the decision-makers can maintain reliability by taking corrective actions, for example, redispatching generation via a security-constrained optimal power flow (SCOPF). Today in operations, real-time CA is run every 5-30 minutes (e.g., ERCOT runs it every 5 min [2] and NERC requires that CA runs at least once every 30 min). Since it is computationally prohibitive to

simulate all combinations of component failures in a limited time, the operators only include a predefined set of N-1 (loss of one component) contingencies in CA. These contingencies correspond to failures due to mechanical issues or natural disasters.

However, today's CA may not suffice when facing a modern grid disturbance in the form of cyberthreat [3]. Unlike N-1 contingencies, cyber threat can cause outages and malicious changes simultaneously at numerous locations, which represents N-k contingencies with $k \gg 1$. Recent years' literature has documented many cyber attack methods of this type [4] [5] [6] [7] [8]. Some of them launch a brute-force attack on many critical control devices (e.g. toggling main breakers of generators), causing blackout for days [5] [6]; some hack into a large set of grid-edge devices (e.g., Internet of Things(IoT) devices) to deny or degrade electric service [8], and some disrupt the confidentiality and integrity of power grid data through the modification of many data values [7].

With the emergence of these cyberthreats, the operators should preemptively secure the grid against them. As such, in the future, CA can be extended to also include cyber events within its predefined set of contingencies. Simulating the power flow impact of these cyber events can inform the grid operators of the grid's susceptibility to cyber attacks, and also filter out potential incidents where preventive actions are needed.

In this paper, we focus on a popular type of cyber threat that can cause N-k contingencies: the MadIoT attack, also called BlackIoT attack, which has emerged due to the proliferation of the Internet of Things (IoT) devices (i.e., grid edge devices). This theoretical attack model succeeds by hacking into the high-wattage IoT-controlled load devices and adversely changing their load demand to disrupt the grid operation. Attack instances of the MadIoT threat represent N-k ($k \gg 1$) events due to the concurrent load manipulations at many locations. Unfortunately, the current computational and analytical techniques in today's CA can hardly solve a large set of N-x contingencies events in an allocated amount of time, like within 30min for real-time CA. The main reason is that, while fast evaluation of N-1 contingencies is possible due to the close proximity of post-contingency solution to the pre-contingency solution, these characteristics no longer hold true for N-k contingencies. Severe N-k contingencies can cause a big shift in the grid states, making it difficult to find good initial conditions that can lead to *robust* and *fast* convergence.

Various techniques can be applied to overcome challenges with fast simulation of N-k contingency events. One option

is to develop contingency screening [9] strategies that can significantly reduce the number of contingencies to simulate. Another option is to develop a warm starter that provides *good* initialization to CA and enables it to converge in fewer iterations. This paper pursues the latter option and proposes a data-driven warm-starter method. Given a pre-contingency network and corresponding contingency information, the warm starter predicts the post-contingency bus voltages. The prediction is then used as the initial point for simulating the contingency.

Developing a data-driven method that is practical for grid-specific application is important. General machine learning (ML) tools for physical systems exhibit drawbacks of requiring massive training data and outputting non-physical solutions. As an improvement, many current works of grid simulation and optimization have explored the use of physics, i.e., domain knowledge or domain expertise, towards developing physics-informed machine learning (ML) approaches. However, we have found that many methods still lack sufficient generalization, interpretability and scalability. Section II-A provides an overview of these current efforts and their limitations.

To address the limitations in the current physics-informed ML methods while developing a data-driven warm starter, this paper builds a probabilistic graphical model where the conditional joint distribution is factorized into a pairwise form. The potential functions (which are components of the factorization) are then defined in the form of Gaussian function, giving rise to a conditional Gaussian Random Field (GRF) to model the conditional joint distribution. Neural networks are used to map from local inputs to the unknown parameters in local Gaussian potential functions, the training of which is based on a maximization of the conditional likelihood. Such an integration of GRF with neural networks aims at improved 1) model generalizability by incorporating topology changes in the grid into the method by using architecture-constrained graphical models, 2) physical interpretability, since the inference model of our Gaussian Random Field has been found to form a linear proxy of the power system, and 3) trainability and scalability by using a graphical model with physics-informed regularization techniques (e.g., parameter sharing). The results show that on a 2000-bus system, the proposed warm starter enabled contingency simulation achieves 5x faster convergence than the traditional initialization methods.

Reproducibility: our code is publicly available at <https://github.com/ohCindy/GridWarm.git>.

II. RELATED WORK

A. Physics-informed ML for power grids: literature review

Many prior works have included domain-knowledge in their methods to address the problem of missing *physics* in generic ML tools. These methods collectively fall under physics-informed ML paradigm for power grid operation, control, and planning and can be broadly categorized into following categories:

1) *Reducing search space:* In these methods, domain knowledge is used to narrow down the search space of parameters and/or solutions. For example, [10] designed a grid topology controller which combines reinforcement learning (RL)

Q-values with power grid simulation to perform a *physics*-guided action exploration, as an alternative to the traditional epsilon-greedy search strategy. Works in [11]- [12] studied the multi-agent RL-based power grid control. In these approaches the power grid is partitioned into controllable sub-regions based on domain knowledge (i.e., electrical characteristics) to reduce the high-dimensional continuous action space into lower-dimension sub-spaces which are easier to handle.

2) *Enforcing system constraints and technical limits:* Many recent works apply deep learning to power grid analysis problems. These include but are not limited to power flow (PF) [13] [14] [15], DC optimal power flow (DCOPF) [16], ACOPF [17] [18] [19] and state estimation (SE) [20] [21] [22]. These methods are generally based on (supervised) learning of an input-to-solution mapping using historical system operational data or synthetic data. One type among these works is unrolled neural networks [20] [21] [22] whose layers mimic the iterative updates to solve SE problems using first-order optimization methods (i.e., gradient descent methods), based on quadratic approximations of the original problem. There are also methods that learn the 'one-step' mapping function. Among these, some use deep neural network (DNN) architectures [13] [14] [17] [16] to learn high-dimensional input-output mappings, some use recurrent neural nets (RNNs) [23] to capture some dynamics, and some apply graph neural networks (GNN) [15] [18] [24] to capture the exact topological structure of power grid. To promote *physical* feasibility of the solution, many works impose equality or inequality system constraints by i) encoding hard constraints inside NN layers (e.g. using sigmoid layer to encode technical limits of upper and lower bounds), ii) applying prior on the NN architecture (e.g., Hamiltonian [25] and Lagrangian neural networks [26]), iii) augmenting the objective function with penalty terms in a supervised [13] or unsupervised [17] [14] way, iv) projecting outputs [16] to the feasible domain, or v) combining many different strategies. In all these methods, incorporating (nonlinear) system constraints remains a challenge, even with state-of-the-art toolboxes [27], and most popular strategies lack rigorous guarantees of nonlinear constraint satisfaction.

While these methods have advanced the state-of-the-art in physics-informed ML for power grid applications, critical limitations in terms of generalization, interpretation, and scalability exist. We discuss these further:

Limited generalization: Many existing methods do not adapt well to changing grid conditions. Take changes in network topology as an example. Many current works are built on non-graphical architectures without any topology-related inputs. These, once trained, only work for one fixed topology and cannot generalize to dynamic grid conditions. More recently, some works have begun to encode topology information. Graph model-based methods (e.g., GNN [15] [18] [24]) naturally impose topology as a hard constraint and thus can account for topology changes. Alternatively, work in [14] encodes the topology information into the penalty term (as a soft constraint) through the admittance and adjacency matrix, and [22] accounts for topology in NN implicitly by applying a topology-based prior through a penalty term. While these methods lead to better topology adaptiveness, they also

have some risks: the use of penalty terms [14] [22] to embed topology information as a soft constraint can lead to limited precision; and, for problems (like OPF) where information needs to be exchanged between far-away graph locations, the use of GNNs requires carefully designed global context vectors to output predictions with global-level considerations.

Limited interpretability: Despite that many ML models (NN, decision trees, K-nearest-neighbors) are universal approximators, interpretations of their functionality from a physically meaningful perspective are still very limited. The general field of *model interpretability* [28] focuses on explaining *how a model works*, to mitigate fears of the unknown. Broadly, investigations of interpretability have been categorized into transparency (also called ad-hoc interpretations) and post-hoc interpretations. The former aims to elucidate the mechanism by which the ML *blackbox* works before any training begins, by considering the notions of *simulatability* (Can a human work through the model from input to output, in reasonable time steps through every calculation required to produce a prediction?), *decomposability* (Can we attach intuitive explanation to each part of a model: each input, parameter, and calculation?), and *algorithmic transparency* (Does the learning algorithm itself confer guarantees on convergence, error surface even for unseen data/problems?). And *post-hoc interpretation* aims to inspect a learned model after training, by considering its natural language explanations, visualizations of learned representations/models, or explanations of empirical examples. However, none of these concepts in the field of ML model interpretability formally evaluates *how a ML model makes predictions in a physically meaningful way* when it is used on an industrial system like the power grid. Some recent works have managed to explore physical meaningfulness of their models from the power system perspective, but interpretations are made in conceptually different ways without uniform metric: Unrolled neural networks (which has been used as data-driven state estimation for power grid [22] [20]) are more decomposable and interpretable in a way that the layers mimic the iterations in the physical solvers, yet these models [21] [20] [22] mainly unroll first-order solvers instead of the second-order (Newton-Raphson) realistic solvers. GNN based models [15] [18] [24] naturally enables better interpretability in terms of representing the graph structure. [13] provides some interpretation of its DNN model for PF, by matching the gradients with power sensitivities and this finding enables accelerating the training by pruning out unimportant gradients. [14] learns a weight matrix that can approximate the bus admittance matrix; however, with only limited precision. To summarize, due to the limited interpretability, ML models still have some opacity and blackbox-ness, when compared with the purely physics-based models (e.g., power flow equations).

Scalability issues: In the case of large-scale systems, models (like DNNs) that learn the mapping from high-dimensional input-output pairs will inevitably require larger and deeper designs of model architecture, and thereafter massive data to learn such mappings. This can affect the practical use in real-world power grid analytics.

3) *Extracting meaningful features or crafting an interpretable latent space:* Many works exist in this class. For

example, [29] [30] learned the latent representation of sensor data in a graph to capture temporal dependency [29] or spatial sensor interactions [30]. [31] applied influence model to learn, for all edge pairs, the pairwise influence matrices which are then used for the prediction of line cascading outages. [32] crafted a graph similarity measure from power sensitivity factors, and detected anomalies in the context of topology changes, by weighing historical data based on this similarity measure.

B. MadIoT: IoT-based Power Grid Cyberthreat

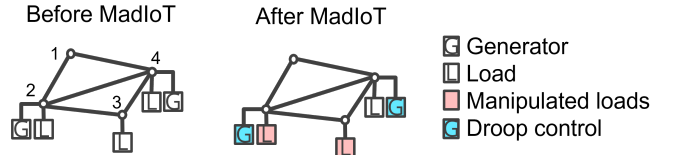


Fig. 1. A toy instance of MadIoT: a subset of loads is manipulated.

The proliferation of IoT devices has raised concerns about IoT-induced cyber attacks. [8] proposed a threat model, namely *BlackIoT* or *MadIoT*, where an attacker can manipulate the power demand by synchronously turning on/off or scaling up/down some high-wattage IoT-controlled loads on the grid. This can lead to grid instability or grid collapse. Figure 1 illustrates an attack instance of the MadIoT threat. To evaluate the impact of a postulated attack, [8] uses steady-state analysis of the power grid while taking into account the droop control, protective relaying, and thermal and voltage limits for various components.

III. A NOVEL WARM STARTER

This paper aims to enable the running of tens of thousands of cyber-threat driven contingencies (C_{N-k}) in a practical amount of time. Purely physics-based solvers can give accurate solutions but are slow when they have to solve a large number of *hard-to-solve* N-k contingency events. In contrast, replacing physical solvers with purely data-driven techniques makes it fast but has severe limitations, as discussed in Section II-A. In this paper, we propose a novel physics-informed ML model that can warm-start the physical solvers when simulating *hard-to-solve* contingencies (C_{N-k}). The warm starter will predict the post-contingency voltages which are supplied as initial conditions to the physical solver for fast convergence. The proposed model is designed to be **generalizable to topology change** by using a graphical model, and **physically interpretable** by forming a linear system proxy, and **scalable** by applying some regularization techniques on the graphical model.

A. Task definition and symbol notations

As shown in Fig. 2, given an input \mathbf{x} which contains contingency information c and (pre-contingency) system information G , a warm starter makes prediction \mathbf{y} which is an estimate of the post-contingency bus voltages \mathbf{v}^{post} . The model is

a function mapping, which is learned from training dataset $Data = \{(\mathbf{x}^{(j)}, \mathbf{y}^{(j)})\}$, where (j) denotes the j -th sample. Table I shows the symbols used in this paper.

TABLE I
SYMBOLS AND DEFINITIONS

Symbol	Interpretation
G	case data before contingency containing topology, generation, and load settings
\mathbf{v}_i	the voltage at bus i , $\mathbf{v}_i = [v_i^{real}, v_i^{imag}]^T$
$\mathbf{v}^{pre/post}$	$\mathbf{v}^{pre/post} = [v_1^{pre/post}, v_2^{pre/post}, \dots, v_n^{pre/post}]^T$ the pre/post-contingency voltages at all buses
c	contingency setting (<i>type, location, parameter</i>) e.g. (<i>MadIoT, [1, 3], 150%</i>) : increasing loads at bus 1 and 3 to 150% the original value.
i, n	bus/node index; total number of nodes
(s, t)	a branch/edge connecting node s and node t
\mathcal{V}, \mathcal{E}	set of all nodes and edges: $i \in \mathcal{V}, \forall i; (s, t) \in \mathcal{E}$
j, N	data sample index; total number of samples
(\mathbf{x}, \mathbf{y})	a sample with feature \mathbf{x} and output \mathbf{y} $\mathbf{y} = [\mathbf{y}_1, \dots, \mathbf{y}_n]^T = [v_1^{post}, \dots, v_n^{post}]^T$

B. Method Overview

Power grid can be naturally represented as a graph, as shown in Fig. 2. Nodes and edges on the graph correspond to power grid buses and branches (lines and transformers), respectively. Each node represents a variable \mathbf{y}_i which denotes voltage phasor at bus i , whereas each edge represents a direct inter-dependency between adjacent nodes.

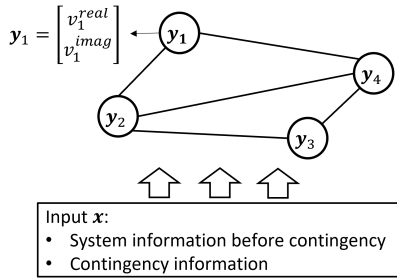


Fig. 2. A Conditional Random Field representing a power grid during contingency: each node represents the bus voltage after contingency, each edge represents a branch status after contingency.

Such a graphical model enables a compact way of writing the conditional joint distribution and performing inference thereafter, using observed data. Specifically, when contingency happens, the joint distribution of variables \mathbf{y} conditioned on input features \mathbf{x} can be factorized in a pairwise manner [33], as (1) shows:

$$P(\mathbf{y}|\mathbf{x}, \boldsymbol{\theta}) = \frac{1}{Z(\boldsymbol{\theta}, \mathbf{x})} \prod_{i=1}^n \psi_i(\mathbf{y}_i) \prod_{(s,t) \in \mathcal{E}} \psi_{st}(\mathbf{y}_s, \mathbf{y}_t) \quad (1)$$

where $\boldsymbol{\theta}$ denotes the model parameter that maps \mathbf{x} to \mathbf{y} ; $\psi_i(\mathbf{y}_i), \psi_{st}(\mathbf{y}_s, \mathbf{y}_t)$ are node and edge potentials conditioned

on $\boldsymbol{\theta}$ and \mathbf{x} ; and $Z(\boldsymbol{\theta}, \mathbf{x})$ is called the partition function that normalizes the probability values such that they sum to the value of 1.

The factorization model in (1) is inspired by pairwise continuous MRF [33] and meanwhile provides good intuition: every edge potential encodes the mutual correlation between two adjacent nodes; both node and edge potentials represent the local contributions of nodes/edges to the joint distribution. In the task of contingency analysis, each potential function intuitively represents how the status of each bus and branch 'independently' impacts the bus voltages.

Given a training dataset of N samples $\{(\mathbf{x}^{(j)}, \mathbf{y}^{(j)})\}$, the training and inference can be described briefly as:

- **Training:** With proper definition of the potential functions $\psi_i(\mathbf{y}_i|\mathbf{x}, \boldsymbol{\theta}), \psi_{st}(\mathbf{y}_s, \mathbf{y}_t|\mathbf{x}, \boldsymbol{\theta})$ (see Section III-C and III-D), and the parameter $\boldsymbol{\theta}$ can be learned by maximizing log-likelihood

$$\hat{\boldsymbol{\theta}} = \arg \max_{\boldsymbol{\theta}} \sum_{j=1}^N \log l(\boldsymbol{\theta})^{(j)} \quad (2)$$

where $l(\boldsymbol{\theta})^{(j)}$ denotes the log-likelihood of the j -th sample

$$l(\boldsymbol{\theta})^{(j)} = P(\mathbf{y}^{(j)}|\mathbf{x}^{(j)}, \boldsymbol{\theta}) \quad (3)$$

- **Inference:** For any new input \mathbf{x}_{test} , we make use of the estimated parameter $\hat{\boldsymbol{\theta}}$ to make a single-point prediction

$$\hat{\mathbf{y}}_{test} = \arg \max_{\mathbf{y}} P(\mathbf{y}|\mathbf{x}_{test}, \hat{\boldsymbol{\theta}}) \quad (4)$$

The use of probabilistic graphical setting naturally integrates the domain knowledge from grid topology into the method:

(Domain knowledge: grid topology) Power flow result is conditioned on the grid topology. Bus voltages of two adjacent buses connected directed by a physical linkage (line or transformer) have direct interactions.

Each sample in this method can have its own topology and each output is conditioned on its input topology. The following sections will further discuss how the graphical model, together with domain knowledge, enables an efficient and physically interpretable model design.

C. Pairwise Conditional Gaussian Random Field

Upon representing the power grid and its contingency as a conditional pairwise MRF factorized in the form of (1), we need to define the potential functions $\psi_i(\mathbf{y}_i), \psi_{st}(\mathbf{y}_s, \mathbf{y}_t)$.

This paper builds a Gaussian random field which equivalently assumes that the output variable (\mathbf{y}) satisfies multivariate Gaussian distribution, i.e., $P(\mathbf{y}|\mathbf{x}, \boldsymbol{\theta})$ is Gaussian. The justification and corresponding benefits of using Gaussian Random Field are:

- partition function $Z(\boldsymbol{\theta}, \mathbf{x})$ is easier to compute due to good statistical properties of Gaussian distribution.
- high physical interpretability due to a physically meaningful inference model. We will discuss this later.

The potential functions for Gaussian random field [33] are defined as follows:

$$\psi_i(\mathbf{y}_i) = \exp\left(-\frac{1}{2}\mathbf{y}_i^T \mathbf{\Lambda}_i \mathbf{y}_i + \boldsymbol{\eta}_i^T \mathbf{y}_i\right) \quad (5)$$

$$\psi_{st}(\mathbf{y}_s, \mathbf{y}_t) = \exp\left(-\frac{1}{2}\mathbf{y}_s^T \mathbf{\Lambda}_{st} \mathbf{y}_t\right) \quad (6)$$

By plugging (5) and (6) into (1), we have:

$$P(\mathbf{y}|\mathbf{x}, \boldsymbol{\theta}) \propto \exp\left(\boldsymbol{\eta}^T \mathbf{y} - \frac{1}{2}\mathbf{y}^T \mathbf{\Lambda} \mathbf{y}\right) \quad (7)$$

where $\mathbf{\Lambda}_i$ and $\mathbf{\Lambda}_{st}$ parameters are the building blocks of matrix $\mathbf{\Lambda}$, and $\boldsymbol{\eta}$ is a column vector composed of all $\boldsymbol{\eta}_i$. To further illustrate, consider a post-contingency grid structure in Fig. 2. The $\boldsymbol{\eta}$ and $\mathbf{\Lambda}$ matrix for this grid structure are shown in Fig. 4 where the $\mathbf{0}$ blocks in $\mathbf{\Lambda}$ matrix are structural zeros representing no edges at the corresponding locations.

In the model (7), both $\boldsymbol{\eta}$ and $\mathbf{\Lambda}$ are functions of $\mathbf{x}, \boldsymbol{\theta}$, i.e.,

$$\boldsymbol{\eta} = f_\eta(\mathbf{x}, \boldsymbol{\theta}_\eta), \mathbf{\Lambda} = f_\Lambda(\mathbf{x}, \boldsymbol{\theta}_\Lambda) \quad (8)$$

and $P(\mathbf{y}|\mathbf{x}, \boldsymbol{\theta})$ takes an equivalent form of a multivariate Gaussian distribution $N(\boldsymbol{\mu}, \boldsymbol{\Sigma})$ ($\boldsymbol{\mu}$ is the mean and $\boldsymbol{\Sigma}$ is the covariance matrix) with

$$\boldsymbol{\eta} = \mathbf{\Lambda} \boldsymbol{\mu}, \mathbf{\Lambda} = \boldsymbol{\Sigma}^{-1} \quad (9)$$

Now based on these defined models, we seek to learn the parameter $\boldsymbol{\theta}$ through maximum likelihood estimation (MLE). The log-likelihood of each data sample can be calculated by:

$$l(\boldsymbol{\theta}) = \log P(\mathbf{y}|\mathbf{x}, \boldsymbol{\theta}) = -\frac{1}{2}\mathbf{y}^T \mathbf{\Lambda} \mathbf{y} + \boldsymbol{\eta}^T \mathbf{y} - \log Z(\boldsymbol{\theta}, \mathbf{x}) \quad (10)$$

and the MLE can be written equivalently as an optimization problem that minimizes the negative log-likelihood loss on the data set of N training samples:

$$\min_{\boldsymbol{\theta}} - \sum_{j=1}^N l(\boldsymbol{\theta})^{(j)} \quad (11)$$

Inference and Interpretation: Upon obtaining the solution of $\hat{\boldsymbol{\theta}} = [\hat{\boldsymbol{\theta}}_\eta, \hat{\boldsymbol{\theta}}_\Lambda]^T$, parameters $\hat{\mathbf{\Lambda}} = f_\Lambda(\mathbf{x}_{test}, \hat{\boldsymbol{\theta}})$, $\hat{\boldsymbol{\eta}} = f_\eta(\mathbf{x}_{test}, \hat{\boldsymbol{\theta}})$ can be estimated thereafter. Then for any test contingency sample \mathbf{x}_{test} , the inference model in (4) is equivalent to solving $\hat{\mathbf{y}}_{test}$ by:

$$\hat{\mathbf{\Lambda}} \hat{\mathbf{y}}_{test} = \hat{\boldsymbol{\eta}} \quad (12)$$

Notably, the model in (12) can be seen as a **linear system approximation** of the post-contingency grid, providing a physical interpretation of the method. $\mathbf{\Lambda}$ is a sparse matrix with similar structure as the bus admittance matrix where the zero entries are 'structural zeros' representing that there is no branch connecting buses. $\boldsymbol{\eta}$ behaves like the net injection to the network.

D. NN-node and NN-edge

Finally to implement the model, we need to specify the functions of $f_\eta(\mathbf{x}, \boldsymbol{\theta}_\eta), f_\Lambda(\mathbf{x}, \boldsymbol{\theta}_\Lambda)$. Taking advantage of the sparsity of $\mathbf{\Lambda}$, the task here is to learn a function mapping from input \mathbf{x} to only some edge-wise parameters $\mathbf{\Lambda}_{st}$ and node-wise parameters $\mathbf{\Lambda}_i, \boldsymbol{\eta}_i$. Yet the number of $\mathbf{\Lambda}_i, \mathbf{\Lambda}_{st}, \boldsymbol{\eta}_i$

parameters still increases with grid size, meaning that the input and output size of the model will explode for a large-scale system, requiring a much more complicated model to learn a high-dimensional input-output map.

To efficiently reduce the model size, this paper implements the mapping functions using local Neural Networks: each node has a *NN-node* to predict $\mathbf{\Lambda}_i, \boldsymbol{\eta}_i$ using local inputs; each edge has *NN-edge* to output $\mathbf{\Lambda}_{st}$ in a similar way, as Figure 3 shows. This is inspired by our interpretation that $\mathbf{\Lambda}$ is a proxy of the bus admittance matrix whose elements represent some local system characteristics regarding each node and edge.

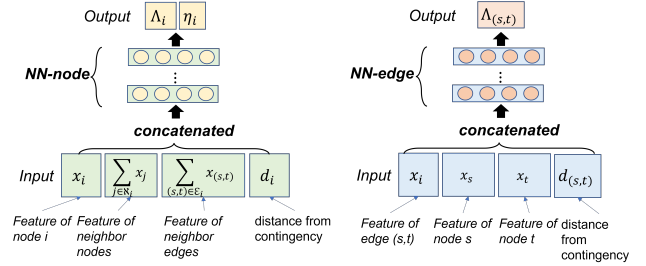


Fig. 3. each node has a *NN-node* and each edge has a *NN-edge*, to map the input features to the post-contingency system characteristics.

Meanwhile, to effectively learn the mapping, we must answer the following question: **how shall we select the input features to the NN models?** We apply *domain knowledge* to design the input space that feeds most relevant features into the model:

(Domain knowledge: decisive features) The impact of contingency depends heavily on the importance of contingency components which can be quantified by the amount of its generation, load or power delivery.

(Domain knowledge: Taylor expansion on system physics) Let $v = h(G)$ denote any power flow simulation that maps from the case information to the voltage profile solution. By Taylor Expansion, the post-contingency voltage can be expressed as a function depending on pre-contingency system G_{pre} and the system change ΔG caused by contingency:

$$\mathbf{v}^{post} = h(G_{pre}) + h'(G_{pre})\Delta G + \frac{1}{2}h''(G_{pre})\Delta G^2 + \dots$$

Therefore, the key features of pre-contingency system and system change are selected as node features to feed into the NN mappings, which are,

- node feature \mathbf{x}_i : $v_i^{real}, v_i^{imag}, P_i, Q_i, I_i^{real}, I_i^{imag}, Q_{shunt,i}$ before contingency, and $\Delta P_{gen,i}, \Delta P_{load,i}, \Delta Q_{load,i}$ caused by contingency
- edge feature $\mathbf{x}_{s,t}$: admittance and shunt capacity of the 'pi-model', $\mathbf{x}_{s,t} = [G, B, B_{sh}]$

E. Training the model with a surrogate loss

With the conditional GRF model defined in Section III-C and the NN models designed in Section III-D, the training process is illustrated in Fig. 4, where the forward pass of NN-node and NN-edge gives $\mathbf{\Lambda}, \boldsymbol{\eta}$, and then the loss defined from

the cGRF can be calculated to further enable a backward pass that updates the parameter θ .

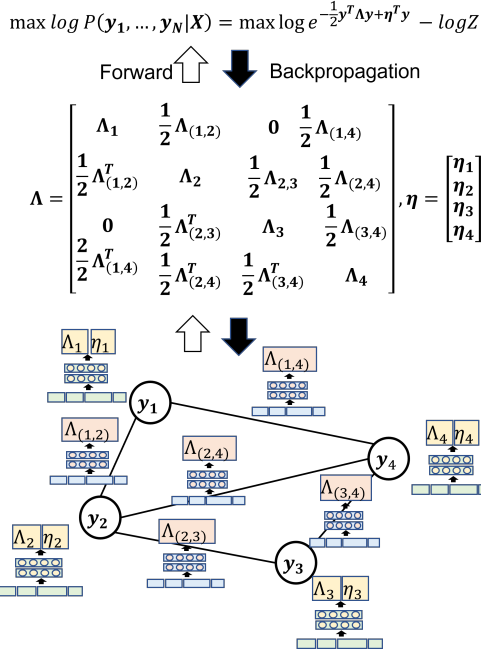


Fig. 4. Training of the proposed method: forward pass and back-propagation.

As described in (10)-(11), the loss function is the negative log-likelihood loss over the training data. Making use of the nice properties of Gaussian distribution, the partition function $Z(\mathbf{x}, \boldsymbol{\theta})$ in the loss can be calculated analytically:

$$\begin{aligned} Z &= \int_{\mathbf{y}} \exp(\boldsymbol{\eta}^T \mathbf{y} - \frac{1}{2} \mathbf{y}^T \Lambda \mathbf{y}) d\mathbf{y} \\ &= \sqrt{\frac{2\pi}{|\Lambda|}} \exp(\frac{\boldsymbol{\mu}^T \Lambda \boldsymbol{\mu}}{2}) = \sqrt{\frac{2\pi}{|\Lambda|}} \exp(\frac{\boldsymbol{\eta}^T \Lambda^{-1} \boldsymbol{\eta}}{2}) \end{aligned} \quad (13)$$

The detailed derivation can be found in Appendix A.

Furthermore, to enable a valid distribution $P(\mathbf{y} | \mathbf{x}, \boldsymbol{\theta})$ and unique solution during inference, it is required that the Λ matrix is positive definite (PD), i.e., $\Lambda \succ \mathbf{0}$. Therefore, adding this constraint and substituting (13) into the loss function, the optimization problem of the proposed method can be written as:

$$\begin{aligned} \min_{\boldsymbol{\theta}} \sum_{j=1}^N \frac{1}{2} \mathbf{y}^{(j)T} \Lambda^{(j)} \mathbf{y}^{(j)} \\ - \boldsymbol{\eta}^{(j)T} \mathbf{y}^{(j)} - \frac{1}{2} \log |\Lambda^{(j)}| + \frac{1}{2} \boldsymbol{\eta}^{(j)T} \Lambda^{-1(j)} \boldsymbol{\eta}^{(j)} \end{aligned} \quad (14)$$

s.t.

$$\text{(forward pass)} \quad \Lambda^{(j)} = f_{\Lambda}(\mathbf{x}^{(j)}, \boldsymbol{\theta}_{\Lambda}), \forall j \quad (15)$$

$$\text{(forward pass)} \quad \boldsymbol{\eta}^{(j)} = f_{\eta}(\mathbf{x}^{(j)}, \boldsymbol{\theta}_{\eta}), \forall j \quad (16)$$

$$\text{(positive definiteness)} \quad \Lambda^{(j)} \succ \mathbf{0}, \forall j \quad (17)$$

In this problem, maintaining the positive definiteness of matrix Λ for every sample is required, not only in the final solution, but throughout the training process (due to the $\log |\Lambda|$ in the loss). Yet this can be very hard especially when the

matrix size is large, making the optimization problem hard-to-solve.

To address this issue, we design a **surrogate loss** which acts as a proxy for the actual loss we want to minimize. With the use of surrogate loss function, the overall problem converts into the following form:

$$\min_{\boldsymbol{\theta}} \sum_{j=1}^N \frac{1}{2} (\mathbf{y}^{(j)} - \boldsymbol{\mu}^{(j)})^T (\mathbf{y}^{(j)} - \boldsymbol{\mu}^{(j)}) \quad (18)$$

s.t.

$$\text{(forward pass)} \quad \Lambda^{(j)} = f_{\Lambda}(\mathbf{x}^{(j)}, \boldsymbol{\theta}_{\Lambda}), \forall j \quad (19)$$

$$\text{(forward pass)} \quad \boldsymbol{\eta}^{(j)} = f_{\eta}(\mathbf{x}^{(j)}, \boldsymbol{\theta}_{\eta}), \forall j \quad (20)$$

$$\text{(inference)} \quad \boldsymbol{\mu}^{(j)} = \Lambda^{-1(j)} \boldsymbol{\eta}^{(j)}, \forall j \quad (21)$$

Appendix B shows how the new loss mathematically approximates the original objective function. In this way, we removed the need to maintain positive-definiteness of the Λ in the learning process, whereas the prediction is made using a Λ computed from the forward pass, and thus it still considers the power grid structure enforced by the graphical model.

From decision theory, both the original and the surrogate loss aim to return an optimized model whose prediction $\hat{\mathbf{y}}$ approximates the ground truth \mathbf{y} , and both make predictions by finding out the linear approximation of the post-contingency system $\hat{\Lambda} \hat{\mathbf{y}} = \hat{\boldsymbol{\eta}}$.

Additionally, this surrogate optimization model can be considered as minimizing the mean squared error (MSE) loss $\frac{1}{2} \|\mathbf{y} - \hat{\mathbf{y}}\|^2$ over the training data, where $\hat{\mathbf{y}}$ is the prediction (inference) made after a forward pass.

IV. INCORPORATING MORE PHYSICS

A. Parameter sharing: a powerful regularizer

With each node having its own *NN-node* and each edge having its *NN-edge*, the number of parameters grows approximately linearly with grid size (more specifically, the number of nodes and edges). Can we reduce the model size further? The answer is yes! One option is to make all nodes share the same *NN-node* and all edges share the same *NN-edge*, so that there are only two NNs in total.

Why does this work? Such sharing of *NN-node* and *NN-edge* is an extensive use of **parameter sharing** to incorporate a domain knowledge into the network. Specially, from the physical perspective:

(Domain knowledge: location-invariant (LI) properties) the power grid and the impact of its contingencies have properties that are invariant to change of locations: 1) any location far enough from the contingency location will experience little local change. 2) change in any location will be governed by the same mechanism, i.e., the system equations.

The use of parameter sharing across the grid significantly lowered the number of unique model parameters, and also reduced the need for a large increase in training data to adequately learn the system mapping for larger grid sizes (like the networks representing continental U.S. network).

B. Zero-injection bus

(Domain knowledge: zero-injection (ZI) buses) A bus with no generation or load connected is called a zero-injection (ZI) bus. These buses neither consume or produce power, and thus injections at these buses are zero.

In the proposed approach, the model parameter η serves as a proxy to bus injections; therefore, we can integrate domain knowledge about zero-injection nodes into the method by setting $\eta_i = 0$ at any ZI node i .

V. EXPERIMENTS

This section runs experiments for instances of CA in the context of a MadIoT attack. The goal is to validate that the proposed warm starter provides good initial states for *hard-to-solve* N-k contingencies and enables faster convergence when compared to traditional initialization techniques.

We test three versions of the proposed method, see Table III. These versions differ in the level of domain-knowledge that they incorporate within their model. Table II summarizes the domain-knowledge in these versions. Table III categorizes the domain knowledge in each version.

TABLE II
SUMMARY OF DOMAIN KNOWLEDGE

Knowledge	Technique	Benefits
topology	graphical model	- physical interpretability - generalization (to topology)
decisive features	feature selection	- accuracy - physical interpretability - generalization (to load&gen)
taylor expansion	feature selection	- accuracy - physical interpretability
LI properties	parameter sharing (PS)	- trainability, scalability - generalization (\downarrow overfitting)
ZI bus	enforce $\eta_i = 0$	- physical interpretability - generalization

TABLE III
CATEGORIZATION OF DOMAIN-KNOWLEDGE IN THE 3 VERSIONS

Knowledge & techniques	cGRF	cGRF-PS	cGRF-PS-ZI
graphical model (cGRF)	✓	✓	✓
feature selection	✓	✓	✓
parameter sharing (PS)		✓	✓
ZI buses			✓

A. Data generation and experiment settings

We generate synthetic MadIoT contingencies for the following two networks: i) IEEE 118 bus network ii) ACTIVSg2000 network. The three-step algorithm we used to generate the synthetic contingency data is given in Algorithm 1.

The experiment settings that are used for the data generation, model design, and model training are documented in Table IV. In our experiment, the model is designed with a shallow 3-layer NN architecture to save computation time and reduce overfitting. It further allows us to experiment on whether a simple model design can give good performance.

Algorithm 1: 3-Step Data Generation Process

Input: Base case G_{base} , type of contingency t_c , number of data samples N_{data}

Output: Generated dataset $\{(x^{(j)}, y^{(j)})\}_{N_{data}}$

- 1 **for** $j \leftarrow 1$ to N_{data} **do**
- 2 **1. Create a random feasible pre-contingency**
 case $G_{pre}^{(j)}$: each sample has random topology, generation and load level.
- 3 **2. Create contingency** $c^{(j)}$ **on** $G_{pre}^{(j)}$: which has attributes *type, location, parameter*.
- 4 **3. Simulate with droop control:** run power flow to obtain the post-contingency voltages v^{post}

TABLE IV
EXPERIMENT SETTINGS

Settings	
N_{data}	case118: 1,000; ACTIVSg2000: 5,000 split into train, val, test set by 8 : 1 : 1
NN -node & NN -edge	shallow cylinder architecture ($n_{layer}, hidden_{dim}$) = (3, 64)
contingency c	<i>type</i> : MadIoT <i>location</i> : randomly sampled 50% loads <i>parameter</i> : case118 200%, ACTIVSg2000 120%
optimizer	<i>Adam</i> , $lr = 0.001$, <i>scheduler</i> = <i>stepLR</i>

B. Training the Model

C. Physical Interpretability

Fig. 6 validates our hypothesis in Section III-C about *the physical interpretation of our method as a linear system proxy*. In the result (see Fig. 6), we show the similarity between the linear proxy given by model parameters Λ, η and the true post-contingency system linearized admittance matrix Y_{bus} and injection current vector J at the solution; thus, validating that the model acts as a linear proxy for the post-contingency operating condition.

D. Application-level practicality

To verify the effectiveness of the warm starter, we compare the convergence speed (# iterations) with three different initialization methods for the physical solver [34]:

- 1) flat start (flat)
- 2) pre-contingency solution (V_{pre})
- 3) physical solver warm-started by the three versions of the proposed method (cGRF)

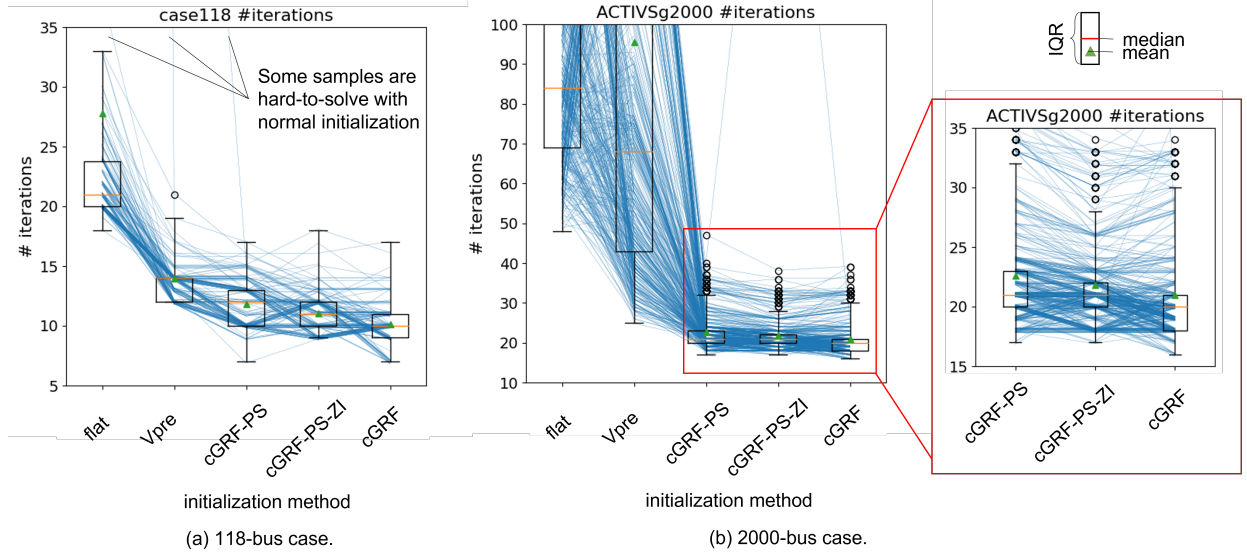


Fig. 5. Result on test data: power flow simulation takes fewer iterations to converge with the proposed method, than traditional initialization methods 1) flat start: starting from all ones; 2) Vpre start: starting from pre-contingency voltages.

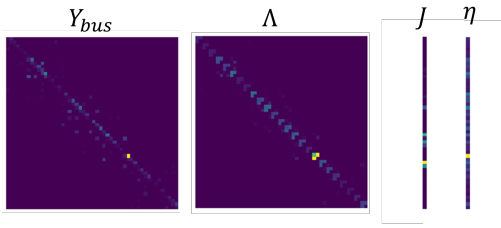


Fig. 6. Physical interpretation: model parameters Λ, η mimic the true post-contingency system admittance matrix Y_{bus} and injection current vector J .

Fig. 5 shows the evaluation results on test data. For cGRF results, we feed the ML predictions into a *robust* power flow simulator: SUGAR [34]. The simulator is robust because it always ensures convergence. In case the general NR loop fails, the simulator uses homotopy to ensure convergence. If the network is infeasible, it identifies that.

The result shows that simulation takes fewer iterations to converge with the proposed ML-based cGRF initialization when compared to traditional initialization methods (flat or V_{pre}). In particular, on ACTIVSg2000, many contingency samples are hard-to-solve with traditional initialization (and may require the homotopy option in SUGAR). In contrast, our ML-based cGRF method significantly speeds up convergence (up to 5x improvement in speed) even with the shallow 3-layer NN architecture.

Moreover, we show that the *lightweight* model cGRF-PS significantly reduces the total number of model parameters but achieves comparable results to the base model cGRF. And cGRF-PS-ZI further shows that integrating more grid physics into the model through zero injection (ZI) knowledge can further improve convergence of the lightweight model.

VI. CONCLUSION

This paper proposes a novel physics-informed ML-based warm starter for cyberthreat-focused contingency analysis. Our

method has the following features:

- **generalizability to topology changes** by using a graphical model to naturally represent grid structure
- **physically interpretability** by generating 'global' predictions from a system-level linear proxy
- **scalability** by using the graphical model and parameter sharing techniques

While being generic in its approach, the method is designed to speed up the simulation of $N - k$ contingency events. We believe these contingencies will be included in the future to evaluate the grid's vulnerability to cyberthreat instances, such as those from the MadIoT attack. In the results, we show that the proposed method can reduce the simulation iteration count by up to 5x, when compared with traditional initialization methods for such contingencies.

ACKNOWLEDGMENT

Work in this paper is supported in part by C3.ai Inc. and Microsoft Corporation.

REFERENCES

- [1] V. J. Mishra and M. D. Khardennis, "Contingency analysis of power system," in *2012 IEEE Students' Conference on Electrical, Electronics and Computer Science*. IEEE, 2012, pp. 1–4.
- [2] X. Li, P. Balasubramanian, M. Sahraei-Ardakani, M. Abdi-Khorsand, K. W. Hedman, and R. Podmore, "Real-time contingency analysis with corrective transmission switching-part i: methodology," *arXiv preprint arXiv:1604.05570*, 2016.
- [3] B. Singer, A. Pandey, S. Li, L. Bauer, C. Miller, L. Pileggi, and V. Sekar, "Shedding light on inconsistencies in grid cybersecurity: Disconnects and recommendations," in *2023 IEEE Symposium on Security and Privacy (SP)*. IEEE Computer Society, 2022, pp. 554–571.
- [4] N. Perloth, "Hackers are targeting nuclear facilities, homeland security dept. and fbi say," *New York Times*, vol. 6, 2017.
- [5] D. U. Case, "Analysis of the cyber attack on the ukrainian power grid," *Electricity Information Sharing and Analysis Center (E-ISAC)*, vol. 388, 2016.
- [6] R. M. Lee, M. Assante, and T. Conway, "Crashoverride: Analysis of the threat to electric grid operations," *Dragos Inc., March*, 2017.

- [7] G. Liang, J. Zhao, F. Luo, S. R. Weller, and Z. Y. Dong, "A review of false data injection attacks against modern power systems," *IEEE Transactions on Smart Grid*, vol. 8, no. 4, pp. 1630–1638, 2016.
- [8] S. Soltan, P. Mittal, and H. V. Poor, "{BlackIoT}:[IoT] botnet of high wattage devices can disrupt the power grid," in *27th USENIX Security Symposium (USENIX Security 18)*, 2018, pp. 15–32.
- [9] S. Li, A. Pandey, and L. Pileggi, "Circuit-theoretic line outage distribution factor," *arXiv preprint arXiv:2204.07684*, 2022.
- [10] T. Lan, J. Duan, B. Zhang, D. Shi, Z. Wang, R. Diao, and X. Zhang, "Ai-based autonomous line flow control via topology adjustment for maximizing time-series atcs," in *2020 IEEE Power & Energy Society General Meeting (PESGM)*. IEEE, 2020, pp. 1–5.
- [11] S. Wang, J. Duan, D. Shi, C. Xu, H. Li, R. Diao, and Z. Wang, "A data-driven multi-agent autonomous voltage control framework using deep reinforcement learning," *IEEE Transactions on Power Systems*, vol. 35, no. 6, pp. 4644–4654, 2020.
- [12] M. Kamruzzaman, J. Duan, D. Shi, and M. Benidris, "A deep reinforcement learning-based multi-agent framework to enhance power system resilience using shunt resources," *IEEE Transactions on Power Systems*, vol. 36, no. 6, pp. 5525–5536, 2021.
- [13] Y. Yang, Z. Yang, J. Yu, B. Zhang, Y. Zhang, and H. Yu, "Fast calculation of probabilistic power flow: A model-based deep learning approach," *IEEE Transactions on Smart Grid*, vol. 11, no. 3, pp. 2235–2244, 2019.
- [14] X. Hu, H. Hu, S. Verma, and Z.-L. Zhang, "Physics-guided deep neural networks for power flow analysis," *IEEE Transactions on Power Systems*, vol. 36, no. 3, pp. 2082–2092, 2020.
- [15] B. Donon, B. Donnot, I. Guyon, and A. Marot, "Graph neural solver for power systems," in *2019 International Joint Conference on Neural Networks (IJCNN)*, 2019, pp. 1–8.
- [16] X. Pan, T. Zhao, and M. Chen, "Deepopf: Deep neural network for dc optimal power flow," in *2019 IEEE International Conference on Communications, Control, and Computing Technologies for Smart Grids (SmartGridComm)*. IEEE, 2019, pp. 1–6.
- [17] P. L. Donti, D. Rolnick, and J. Z. Kolter, "Dc3: A learning method for optimization with hard constraints," *arXiv preprint arXiv:2104.12225*, 2021.
- [18] D. Owerko, F. Gama, and A. Ribeiro, "Optimal power flow using graph neural networks," in *ICASSP 2020 - 2020 IEEE International Conference on Acoustics, Speech and Signal Processing (ICASSP)*, 2020, pp. 5930–5934.
- [19] F. Diehl, "Warm-starting ac optimal power flow with graph neural networks," in *33rd Conference on Neural Information Processing Systems (NeurIPS 2019)*, 2019, pp. 1–6.
- [20] L. Zhang, G. Wang, and G. B. Giannakis, "Real-time power system state estimation via deep unrolled neural networks," in *2018 IEEE Global Conference on Signal and Information Processing (GlobalSIP)*, 2018, pp. 907–911.
- [21] —, "Real-time power system state estimation and forecasting via deep unrolled neural networks," *IEEE Transactions on Signal Processing*, vol. 67, no. 15, pp. 4069–4077, 2019.
- [22] Q. Yang, A. Sadeghi, G. Wang, G. B. Giannakis, and J. Sun, "Gauss-newton unrolled neural networks and data-driven priors for regularized psse with robustness," *arXiv preprint arXiv:2003.01667*, 2020.
- [23] N. Yadaiah and G. Sowmya, "Neural network based state estimation of dynamical systems," in *The 2006 IEEE international joint conference on neural network proceedings*. IEEE, 2006, pp. 1042–1049.
- [24] O. Kundacina, M. Cosovic, and D. Vukobratovic, "State estimation in electric power systems leveraging graph neural networks," *arXiv preprint arXiv:2201.04056*, 2022.
- [25] S. Greydanus, M. Dzamba, and J. Yosinski, "Hamiltonian neural networks," *Advances in Neural Information Processing Systems*, vol. 32, 2019.
- [26] M. Lutter, C. Ritter, and J. Peters, "Deep lagrangian networks: Using physics as model prior for deep learning," *arXiv preprint arXiv:1907.04490*, 2019.
- [27] A. Tuor, J. Drgona, and M. Skomski, "NeuroMANCER: Neural Modules with Adaptive Nonlinear Constraints and Efficient Regularizations," 2022. [Online]. Available: <https://github.com/pnnl/neuromancer>
- [28] Z. C. Lipton, "The mythos of model interpretability: In machine learning, the concept of interpretability is both important and slippery," *Queue*, vol. 16, no. 3, pp. 31–57, 2018.
- [29] Y. Yuan, Y. Guo, K. Dehghanpour, Z. Wang, and Y. Wang, "Learning-based real-time event identification using rich real pmu data," *IEEE Transactions on Power Systems*, vol. 36, no. 6, pp. 5044–5055, 2021.
- [30] Y. Yuan, Z. Wang, and Y. Wang, "Learning latent interactions for event identification via graph neural networks and pmu data," *arXiv preprint arXiv:2010.01616*, 2020.
- [31] X. Wu, D. Wu, and E. Modiano, "An influence model approach to failure cascade prediction in large scale power systems," in *2020 American Control Conference (ACC)*, 2020, pp. 4981–4988.
- [32] S. Li, A. Pandey, B. Hooi, C. Faloutsos, and L. Pileggi, "Dynamic graph-based anomaly detection in the electrical grid," *IEEE Transactions on Power Systems*, 2021.
- [33] K. P. Murphy, "Undirected graphical models (markov random fields)," *Machine Learning: A Probabilistic Perspective*; MIT Press: Cambridge, MA, USA, pp. 661–705, 2012.
- [34] A. Pandey, M. Jereminov, M. R. Wagner, D. M. Bromberg, G. Hug, and L. Pileggi, "Robust power flow and three-phase power flow analyses," *IEEE Transactions on Power Systems*, vol. 34, no. 1, pp. 616–626, 2018.

APPENDIX

A. Calculate partition function

For a multivariate Gaussian distribution $\mathbf{y} \sim N(\boldsymbol{\mu}, \boldsymbol{\Sigma})$ where $\boldsymbol{\mu}$ denotes the mean and $\boldsymbol{\Sigma}$ denotes the covariance matrix, let $\boldsymbol{\Lambda} = \boldsymbol{\Sigma}^{-1}$, we have:

$$\int_{\mathbf{y}} \sqrt{\frac{|\boldsymbol{\Lambda}|}{2\pi}} \exp\left(-\frac{1}{2}(\mathbf{y} - \boldsymbol{\mu})^T \boldsymbol{\Lambda}(\mathbf{y} - \boldsymbol{\mu})\right) d\mathbf{y} = 1 \quad (22)$$

As mentioned earlier, the Gaussian CRF model $P(\mathbf{y}|\mathbf{x}, \boldsymbol{\theta}) = \frac{1}{Z(\mathbf{x}, \boldsymbol{\theta})} \exp(\boldsymbol{\eta}^T \mathbf{y} - \frac{1}{2} \mathbf{y}^T \boldsymbol{\Lambda} \mathbf{y})$ is equivalent to a multivariate Gaussian distribution $N(\boldsymbol{\mu}, \boldsymbol{\Sigma})$ with $\boldsymbol{\eta} = \boldsymbol{\Lambda} \boldsymbol{\mu}$, $\boldsymbol{\Lambda} = \boldsymbol{\Sigma}^{-1}$. Thus (22) can be rewritten as:

$$\sqrt{\frac{|\boldsymbol{\Lambda}|}{2\pi}} \exp\left(-\frac{\boldsymbol{\mu}^T \boldsymbol{\Lambda} \boldsymbol{\mu}}{2}\right) \int_{\mathbf{y}} \exp(\boldsymbol{\eta}^T \mathbf{y} - \frac{1}{2} \mathbf{y}^T \boldsymbol{\Lambda} \mathbf{y}) d\mathbf{y} = 1 \quad (23)$$

Taking the nice properties of Gaussian distribution, the partition function $Z(\mathbf{x}, \boldsymbol{\theta})$ can be calculated as:

$$Z(\mathbf{x}, \boldsymbol{\theta}) = \int_{\mathbf{y}} \exp(\boldsymbol{\eta}^T \mathbf{y} - \frac{1}{2} \mathbf{y}^T \boldsymbol{\Lambda} \mathbf{y}) d\mathbf{y} = \sqrt{\frac{2\pi}{|\boldsymbol{\Lambda}|}} \exp\left(\frac{\boldsymbol{\mu}^T \boldsymbol{\Lambda} \boldsymbol{\mu}}{2}\right) \quad (24)$$

B. Surrogate loss

Mathematically, due to the Gaussian distribution properties, the original optimization problem in (17) is equivalently:

$$\min_{\boldsymbol{\theta}} \sum_{j=1}^N \frac{1}{2} (\mathbf{y}^{(j)} - \boldsymbol{\mu}^{(j)})^T \boldsymbol{\Lambda}^{(j)} (\mathbf{y}^{(j)} - \boldsymbol{\mu}^{(j)}) - \frac{1}{2} \log |\boldsymbol{\Lambda}^{(j)}| \quad (25)$$

s.t.

$$\text{(forward pass)} \quad \boldsymbol{\Lambda}^{(j)} = f_{\boldsymbol{\Lambda}}(\mathbf{x}^{(j)}, \boldsymbol{\theta}_{\boldsymbol{\Lambda}}), \forall j \quad (26)$$

$$\text{(forward pass)} \quad \boldsymbol{\eta}^{(j)} = f_{\boldsymbol{\eta}}(\mathbf{x}^{(j)}, \boldsymbol{\theta}_{\boldsymbol{\eta}}), \forall j \quad (27)$$

$$\text{(positive definiteness)} \quad \boldsymbol{\Lambda}^{(j)} \succ \mathbf{0}, \forall j \quad (28)$$

$$\text{(inference)} \quad \boldsymbol{\mu}^{(j)} = \boldsymbol{\Lambda}^{-1(j)} \boldsymbol{\eta}^{(j)}, \forall j \quad (29)$$

To design a surrogate loss, we make an approximation $\boldsymbol{\Lambda}^{(j)} = \mathbf{I}$ (\mathbf{I} is identity matrix) only in the objective function, so that $\log |\boldsymbol{\Lambda}| = 0$ becomes negligible.